*J Physiol* 595.16 (2017) pp 5699–5712



The Journal of Physiology

# EEA1 restores homeostatic synaptic plasticity in hippocampal neurons from Rett syndrome mice

Xin Xu and Lucas Pozzo-Miller

*Department of Neurobiology, Civitan International Research Center, University of Alabama at Birmingham, Birmingham, AL 35294, USA*

**Key points**

- Rett syndrome is a neurodevelopmental disorder caused by loss-of-function mutations in *MECP2*, the gene encoding the transcriptional regulator methyl-CpG-binding protein 2 (MeCP2). *Mecp2* deletion in mice results in an imbalance of excitation and inhibition in hippocampal neurons, which affects 'Hebbian' synaptic plasticity.
- We show that *Mecp2*-deficient neurons also lack homeostatic synaptic plasticity, likely due to reduced levels of EEA1, a protein involved in AMPA receptor endocytosis.
- Expression of EEA1 restored homeostatic synaptic plasticity in *Mecp2*-deficient neurons, providing novel targets of intervention in Rett syndrome.

**Abstract** Rett syndrome is a neurodevelopmental disorder caused by loss-of-function mutations in *MECP2*, the gene encoding the transcriptional regulator methyl-CpG-binding protein 2 (MeCP2). Deletion of *Mecp2* in mice results in an imbalance of synaptic excitation and inhibition in hippocampal pyramidal neurons, which affects 'Hebbian' long-term synaptic plasticity. Since the excitatory–inhibitory balance is maintained by homeostatic mechanisms, we examined the role of MeCP2 in homeostatic synaptic plasticity (HSP) at excitatory synapses. Negative feedback HSP, also known as synaptic scaling, maintains the global synaptic strength of individual neurons in response to sustained alterations in neuronal activity. Hippocampal neurons from *Mecp2* knockout (KO) mice do not show the characteristic homeostatic scaling up of the amplitude of miniature excitatory postsynaptic currents (mEPSCs) and of synaptic levels of the GluA1 subunit of AMPA-type glutamate receptors after 48 h silencing with the $Na^+$ channel blocker tetrodotoxin. This deficit in HSP is bidirectional because *Mecp2* KO neurons also failed to scale down mEPSC amplitudes and GluA1 synaptic levels after 48 h blockade of type A GABA receptor ($GABA_AR$)-mediated inhibition with bicuculline. Consistent with the role of synaptic trafficking of AMPA-type of glutamate receptors in HSP, *Mecp2* KO neurons have lower levels of early endosome antigen 1 (EEA1), a protein involved in AMPA-type glutamate receptor endocytosis. In addition, expression of EEA1 in *Mecp2* KO neurons reduced mEPSC amplitudes to wild-type levels, and restored synaptic scaling down of mEPSC amplitudes after 48 h blockade of $GABA_AR$-mediated inhibition with bicuculline. The identification of a molecular deficit in HSP in *Mecp2* KO neurons provides potentially novel targets of intervention for improving hippocampal function in Rett syndrome individuals.

(Received 3 April 2017; accepted after revision 5 June 2017; first published online 16 June 2017)
**Corresponding author** L. Pozzo-Miller: Department of Neurobiology, University of Alabama at Birmingham, 1825 University Blvd, Birmingham, AL 35294, USA. Email: lucaspm@uab.edu

**Abbreviations** AMPAR, AMPA-type glutamate receptor; D-AP5, D-(−)-2-amino-5-phosphonopentanoic acid; CNQX, 6-cyano-7-nitro-quinoxaline-2,3-dione; EEA1, early endosome antigen 1; $GABA_AR$, type A GABA receptor; GFP, green fluorescent protein; GluA1, subunit 1 of AMPA-type glutamate receptor; HSP, homeostatic synaptic plasticity; KO, knockout; MeCP2, methyl-CpG-binding protein 2; mEPSC, miniature excitatory postsynaptic current; mIPSC, miniature inhibitory postsynaptic current; RTT, Rett syndrome; TTX, tetrodotoxin; VGLUT1, vesicular glutamate transporter.



DOI: 10.1113/JP274450

## Introduction

Rett syndrome (RTT) is a neurodevelopmental disorder associated with intellectual disability and autism that almost exclusively affects females, with an incidence of 1:10,000 live births (Neul & Zoghbi, 2004). It is primarily caused by loss-of-function mutations in *MECP2*, the gene encoding the transcriptional regulator methyl-CpG-binding protein 2 (MeCP2) (Nan *et al.* 1997; Amir *et al.* 1999; Percy & Lane, 2005). Numerous studies have revealed dysfunctions at the synaptic, neuronal, network and behavioural levels in *Mecp2*-deficient mice (McGraw *et al.* 2011; Calfa *et al.* 2011*b*). The hippocampus of *Mecp2* knockout (KO) mice is hyperactive due to an imbalance of synaptic excitation and inhibition that results from impaired synaptic inhibition and that also affects synaptic plasticity (Calfa *et al.* 2011*a*; Calfa *et al.* 2015; Li *et al.* 2016). shRNA-mediated knockdown of *Mecp2* also affects homeostatic synaptic plasticity (HSP) in hippocampal neurons (Blackman *et al.* 2012; Qiu *et al.* 2012), but the molecular mechanisms of that deficit remain unexplored.

Negative feedback HSP, also known as synaptic scaling, maintains the global synaptic strength of individual neurons in response to sustained alterations in neuronal activity (Turrigiano *et al.* 1998; Turrigiano & Nelson, 2004; Turrigiano, 2007, 2008). Total synaptic strength is regulated by changes in postsynaptic receptor accumulation, presynaptic transmitter release probability, the number of functional synapses, or a combination of those mechanisms (Turrigiano & Nelson, 2004; Wierenga *et al.* 2005; Turrigiano, 2007, 2008). During HSP at excitatory synapses, surface levels of AMPA-type glutamate receptors (AMPARs) at postsynaptic sites are scaled up or down after chronic silencing or over-excitation by blockade of type A GABA receptor ($GABA_AR$)-mediated inhibition, respectively (Lissin *et al.* 1998; O'Brien *et al.* 1998; Wierenga *et al.* 2005; Blackman *et al.* 2012; Qiu *et al.* 2012; Wang *et al.* 2012). Such changes are not only accompanied by modifications in the turnover and synaptic localization of postsynaptic proteins involved in AMPAR insertion at synapses, but also depend on the relative rates of AMPAR exocytosis and endocytosis (Turrigiano & Nelson, 2004). Early endosome antigen 1 (EEA1), a membrane protein associated with the cytoplasmic face of early endosomes, participates in the endocytosis of neurotransmitter receptors by regulating the fusion of vesicle carrying receptors to the recycling endosome, and is highly expressed in the postsynaptic compartment of hippocampal synapses (Selak *et al.* 2000, 2006). An unbiased gene array study of hypothalamic samples from *Mecp2* KO and *Mecp2* overexpressing mice found that *Eea1* levels are down-regulated in *Mecp2* KO mice (Chahrour *et al.* 2008). Here, we confirmed that EEA1 mRNA and protein levels are lower in the *Mecp2* KO hippocampus, suggesting impaired AMPAR endocytosis. In this study, we tested whether EEA1 expression is able to restore HSP in hippocampal neurons from *Mecp2* KO mice.

## Methods

### Animals

Breeding pairs of mice lacking exon 3 of the X chromosome-linked *Mecp2* gene (B6.Cg-*Mecp2* $^{tm1.1Jae}$, 'Jaenisch' strain in a pure C57BL/6 background) (Chen *et al.* 2001) were purchased from the Mutant Mouse Regional Resource Centre at the University of California, Davis. A colony was established at the University of Alabama at Birmingham (UAB) by mating wild-type (WT) males with heterozygous *Mecp2* $^{tm1.1Jae}$ mutant females, as recommended by the supplier. Genotyping was performed by PCR of DNA samples from tail clips. Hemizygous *Mecp2*$^{tm1.1Jae}$ mutant males (called knockouts, KO) are healthy until 5–6 weeks of age, when they begin to show RTT-like symptoms, such as hypoactivity, hindlimb clasping, reflex impairments and irregular breathing (Chen *et al.* 2001). Animals were handled and housed according to the Committee on Laboratory Animal Resources of the National Institutes of Health, and had *ad libitum* access to food and water; all experimental protocols were reviewed annually and approved by the Institutional Animals Care and Use Committee of the University of Alabama at Birmingham.

### Primary cultures of hippocampal neurons

Postnatal day 0 or 1 male *Mecp2* KO mice and WT littermates were deeply anaesthetized with isoflurane. Both hippocampi were rapidly dissected and dissociated in papain (20 U $ml^{-1}$) plus DNase I (Worthington Biochemical Corp., Lakewood, NJ, USA) for 20–30 min at 37°C, as described (Amaral & Pozzo-Miller, 2007). The tissue was then triturated to obtain a single-cell suspension, and the cells were plated at a density of 40,000 cells $cm^{-2}$ on 18 mm poly-L-lysine/laminin coated glass coverslips, and immersed in Neurobasal medium (Life Technologies, Carlsbad, CA, USA) supplemented with 2% B27 (Life Technologies) and 0.5 mM glutamine (Life Technologies). Neurons were grown in 37°C, 5% $CO_2$, 90% relative humidity incubators (Forma, Thermo Fisher Scientific, Waltham, MA, USA), with half of the fresh medium changed every 3–4 days. After 7–8 days *in vitro* (DIV), neurons were exposed for 48 h to the $Na^+$ channel blocker tetrodotoxin (TTX, 1 $\mu$M; Alomone Labs, Jerusalem, Israel), a combination of the AMPAR receptor antagonist 6-cyano-7-nitro-quinoxaline-2,3-dione (CNQX; 10 $\mu$M, Sigma-Aldrich, St Louis, MO, USA) and the NMDA receptor antagonist D-(−)-2-amino-5-phosphonopentanoic acid (D-AP5; 50 $\mu$M,

Sigma-Aldrich), or the $GABA_A$ receptor antagonist bicuculline (20 $\mu$M; Tocris Bioscience, Minneapolis, MN, USA). All experiments were performed between 9 and 11 DIV.

### Transfections and immunocytochemistry

Neurons were transfected with green fluorescent protein (GFP) using Lipofectamine 2000 (Life Technologies) (1.6 $\mu$g DNA) according to the protocol of the manufacturer. Neurons were fixed 48 h after transfection, with 4% (w/v) paraformaldehyde–sucrose for 10 min, and incubated in 0.25% (v/v) Triton X-100 for 10 min, then washed with phosphate buffered saline (PBS). After blocking with 10% (v/v) goat serum in PBS, cells were incubated with primary antibodies against the GluA1 subunit of AMPA-type glutamate receptors, and the vesicular glutamate transporter (VGLUT1), overnight at 4°C, rinsed in PBS, and incubated with secondary antibodies conjugated to Alexa 594 and Alexa 647 (Jackson ImmunoResearch Laboratories, West Grove, PA, USA), respectively, for 1 h at room temperature. Coverslips were then mounted with Vectashield medium (Vector Laboratories, Burlingame, CA, USA) and imaged in a laser-scanning confocal microscope (Zeiss LSM510, Carl Zeiss Microscopy, LLC, Thornwood, NY, USA) using a ×63 (1.4 NA) oil-immersion objective. Three randomly selected segments of primary or secondary dendrites (30–40 $\mu$m for each segment) were analysed for synaptic density; these dendritic segments were located at least one soma diameter away from the soma, and were void of crossing dendrites and axons from other neurons. Surface GluA1 and presynaptic VGLUT1 levels were quantified by measuring the integrated intensity of co-localized puncta using ImageJ (NIH, Bethesda, MD, USA).

### Electrophysiology

Coverslips were continuously perfused with artificial cerebrospinal fluid (aCSF) containing (in mM): 130 NaCl, 5.4 KCl, 2 $CaCl_2$, 1.2 $MgCl_2$, 20 Hepes, 15 glucose; pH 7.4; 25°C. Miniature excitatory postsynaptic currents (mEPSCs) were recorded in the whole-cell configuration from pyramidal neurons voltage clamped at −70 mV using an Axopatch 200B amplifier (Molecular Devices, Sunnyvale, CA, USA). The intracellular solution contained (in mM): 120 caesium gluconate, 17.5 CsCl, 10 Na-Hepes, 4 Mg-ATP, 0.4 Na-GTP, 10 $Na_2$-creatine phosphate, 0.2 Na-EGTA; pH 7.4; 300 mosmol $l^{-1}$. To pharmacologically isolate mEPSCs, the aCSF contained 0.5 $\mu$M TTX, 50 $\mu$M D-AP5, and 50 $\mu$M picrotoxin (Sigma-Aldrich). Miniature inhibitory postsynaptic currents (mIPSCs) were recorded as inward currents at −70 mV using high $Cl^-$ intracellular solution (130 mM KCl, 10 Na-Hepes, 4 Mg-ATP, 0.4 Na-GTP, 10 $Na_2$-creatine phosphate, 0.2 Na-EGTA; pH 7.4; 300 mosmol $l^{-1}$), and with aCSF containing 0.5 $\mu$M TTX, 50 $\mu$M D-AP5, and 10 $\mu$M CNQX. Whole-cell currents were digitized at 10 kHz and filtered at 2 kHz. Cells with series resistance $>$ 20 MΩ or that changed by $\geq$ 20% during the recording were excluded. mEPSCs and mIPSCs were detected and analysed using the MiniAnalysis program (Synaptosoft, Fort Lee, NJ, USA). Peak-scaled non-stationary noise analysis of mEPSCs was performed in MiniAnalysis.

### Western immunoblotting

Brain tissues including cerebral cortex, hippocampus, striatum, thalamus and brainstem were dissected and homogenized in NP-40 lysis buffer (20 mM Tris at pH 8.0, 137 mM NaCl, 10% glycerol, 1% Nonidet P-40, 2 mM EDTA) containing protease inhibitor. The homogenates were maintained with constant agitation for 2 h at 4°C and centrifuged at 12,000 $g$ for 20 min. The supernatants were aspirated and protein concentrations were determined by the Lowry method. Fifteen micrograms of protein sample from whole homogenates was subjected to SDS-PAGE (Bio-Rad Laboratories, Hercules, CA, USA) and transferred to polyvinylidene fluoride membrane (Milipore, Billerica, MA, USA). Membranes were probed with primary antibody against EEA1 (Cell Signaling Technology, Danvers, MA, USA) and detected using Odyssey infrared imaging system (Li-Cor Biosciences, Lincoln, NE, USA). Loading control was probed with $\beta$-actin (Life Technologies).

### Real time quantitative RT-PCR

Total RNA was extracted using RNeasy Plus Mini Kit (Qiagen, Germantown, MD, USA). RNA concentrations were determined in a NanoDrop spectrophotometer (Thermo Fisher Scientific). mRNA was reverse-transcribed using the iScript cDNA Synthesis Kit (Bio-Rad) according to the manufacturer's instructions. PCR amplifications were performed using iQ SYBR Green Supermix (Bio-Rad) with designed primers. Two replicates were performed for each sample.

### Statistical analyses

All the experiments were performed at least three different times, from at least three different neuronal culture preparations. Data are presented as mean ± standard error of the mean (SEM), and were compared using Student's unpaired $t$ test, one-way ANOVA, or the Kolmogorov–Smirnov (K–S) test using Prism software (GraphPad Software, San Diego, CA, USA). Statistical Power was calculated using G*Power (Faul *et al.* 2007); $P < 0.05$ was considered significant.

## Results

The number of excitatory synapses, identified as VGLUT1-expressing presynaptic terminals apposed to dendritic spines of GFP-expressing neurons, and their surface levels of GluA1 were determined by triple colour immunocytochemistry (Fig. 1*A*). Consistent with previous reports (Chao *et al.* 2007; Baj *et al.* 2014), 7–8 days *in vitro* (DIV) cultured hippocampal neurons from *Mecp2* KO mice had fewer excitatory synapses than WT neurons (Fig. 1*A* and *B*; $P = 0.01$). However, excitatory synapses from *Mecp2* KO mice had significantly higher surface levels of GluA1 ($P = 0.0035$) and VGLUT1 ($P < 0.0001$) than WT neurons (Fig. 1*A*, *C* and *D*), consistent with stronger excitatory synapses (Fig. 2; Li *et al.* 2016).

### Homeostatic scaling of synaptic GluA1 levels is altered in *Mecp2* KO neurons

Synaptic scaling at excitatory synapses is mainly mediated through an alteration in synaptic AMPAR accumulation (Lissin *et al.* 1998; O'Brien *et al.* 1998; Wierenga *et al.* 2005; Wang *et al.* 2012). Therefore, we assessed synaptic scaling via fluorescence intensity of synaptic GluA1 levels. HSP was induced in hippocampal cultures from male *Mecp2* KO and WT littermate pups by either silencing with the $Na^+$ channel blocker TTX (1 $\mu$M) or over-excitation by blockade of $GABA_A$R-mediated inhibition with the selective antagonist bicuculline (20 $\mu$M) for 48 h. Chronic silencing of WT neurons with TTX significantly increased the levels of GluA1 (ANOVA, $P = 0.0003$; Dunnett's *post hoc* test, $P < 0.05$) and VGLUT1 (ANOVA, $P = 0.0004$; Dunnett's *post hoc* test, $P < 0.05$), whereas their over-excitation with bicuculline significantly decreased GluA1 ($P < 0.05$) and VGLUT1 ($P < 0.05$) levels (Fig. 1*A*, *C* and *D*; Ctl, $n = 13$ neurons; TTX, $n = 14$; bicuculline, $n = 9$). Neither chronic silencing nor over-excitation affected the numerical density of VGLUT1/GluA1 puncta on GFP-filled spines of WT neurons (Fig. 1*A* and *B*; ANOVA, $P = 0.7638$). On the other hand, *Mecp2* KO neurons did not show synaptic scaling of GluA1 levels. Instead of scaling up GluA1 levels, chronic silencing with TTX significantly decreased GluA1 (ANOVA, $P = 0.0033$; Dunnett's *post hoc* test, $P < 0.01$) and VGLUT1 (ANOVA,

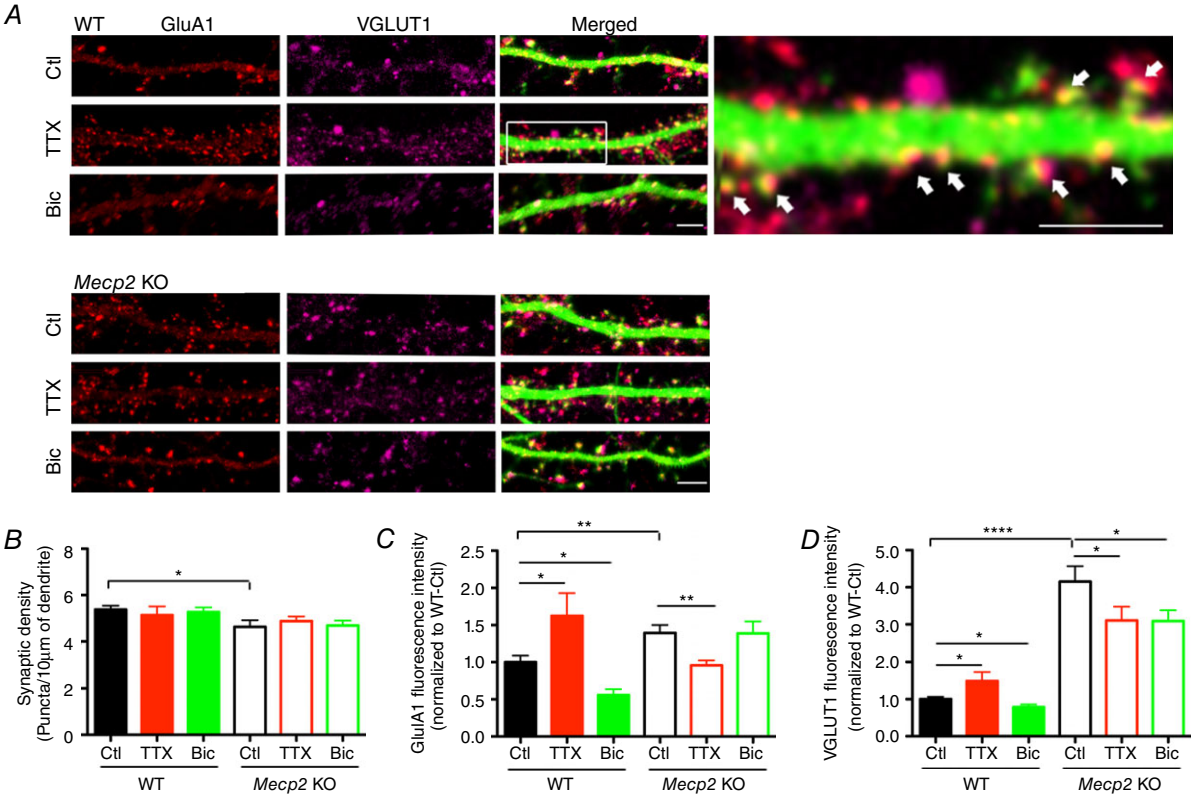


**Figure 1. Synaptic scaling of AMPARs at synapses is altered in *Mecp2* knockout neurons**
*A*, representative images of immunostaining for surface GluA1 (red) and VGLUT1 (purple) in GFP-expressing (green) WT and *Mecp2* KO neurons in Ctl, TTX- or bicuculline-treated cultures (48 h); scale bar: 5 $\mu$m. Excitatory synapses are shown by arrows. *B*, numerical density of GluA1/VGLUT1 synaptic puncta in WT and *Mecp2* KO neurons. *C*, fluorescence intensity of GluA1 synaptic puncta in WT and *Mecp2* KO neurons. *D*, fluorescence intensity of VGLUT1 synaptic puncta in WT and *Mecp2* KO neurons. Fluorescence intensity was normalized to WT neurons in Ctl condition. $^*P < 0.05$; $^{**}P < 0.01$; $^{****}P < 0.0001$. [Colour figure can be viewed at wileyonlinelibrary.com]

$P = 0.0260$; Dunnett's *post hoc* test, $P < 0.05$) levels in *Mecp2* KO neurons (Fig. 1*A*, *C* and *D*; Ctl, $n = 16$; TTX, $n = 16$). In addition, chronic over-excitation with bicuculline did not affect GluA1 levels in *Mecp2* KO neurons (Fig. 1*A* and *C*; bicuculline, $n = 18$; $P > 0.05$). Intriguingly, presynaptic VGLUT1 levels scaled down in *Mecp2* KO neurons after chronic over-excitation, as observed in WT neurons (Fig. 1*A* and *D*; $P < 0.05$). Neither chronic silencing nor over-excitation affected the numerical density of VGLUT1/GluA1 puncta on GFP-filled spines of *Mecp2* KO neurons (Fig. 1*A* and *B*; ANOVA, $P = 0.7478$). These data indicate that homeostatic scaling of synaptic GluA1 levels is altered in hippocampal pyramidal neurons from *Mecp2* KO mice.

## Homeostatic synaptic plasticity is impaired in *Mecp2* KO neurons

We next recorded miniature excitatory postsynaptic currents (mEPSCs) in pyramidal WT and *Mecp2* KO neurons. Consistent with the higher levels of surface GluA1 and presynaptic VGLUT1 levels, mEPSCs were larger ($P = 0.0066$) and more frequent ($P = 0.0324$) in *Mecp2* KO neurons than in WT neurons (Fig. 2). Chronic silencing of WT neurons with TTX for 48 h significantly increased the amplitude (ANOVA, $P = 0.0010$; Dunnett's *post hoc* test, $P < 0.01$) and frequency (ANOVA, $P = 0.0460$; Dunnett's *post hoc* test, $P < 0.05$) of mEPSCs. Similar results were obtained by chronic silencing with a combination

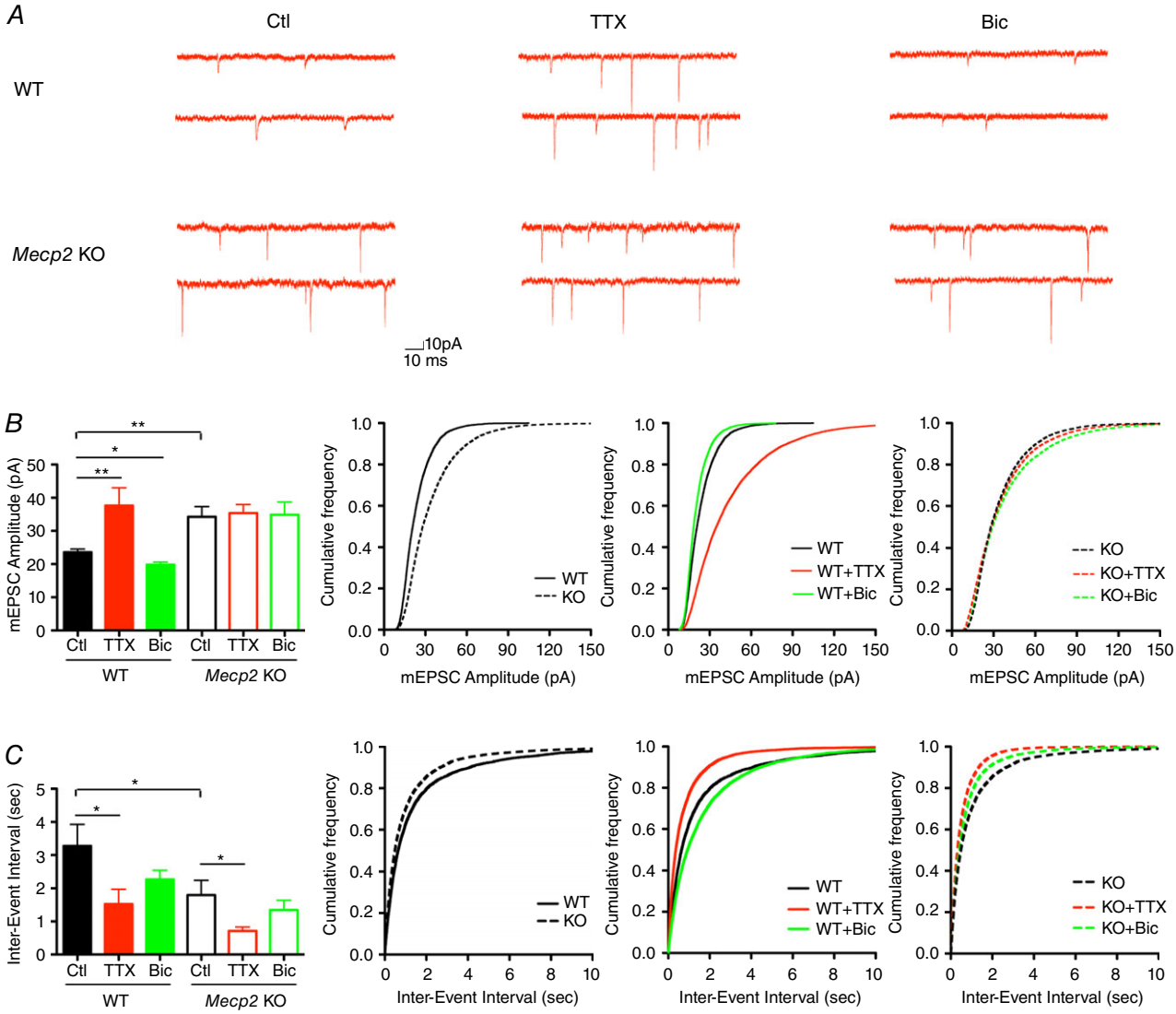


**Figure 2. Homeostatic synaptic plasticity is impaired in *Mecp2* knockout neurons**
*A*, representative mEPSC recordings from WT and *Mecp2* KO neurons in Ctl, TTX- or bicuculline-treated cultures (48 h). *B*, average mEPSC amplitudes (for each cell) and cumulative probability distributions of all mEPSC amplitudes from WT and *Mecp2* KO neurons. *C*, average mEPSC inter-event intervals (for each cell) and cumulative probability distributions of all mEPSC inter-event intervals from WT and *Mecp2* KO neurons. $^*P < 0.05$; $^{**}P < 0.01$. [Colour figure can be viewed at wileyonlinelibrary.com]

**Table 1. Amplitude and inter-event interval of mEPSCs and mIPSCs**

| | | Amplitude | | Inter-Event interval | |
|---|---|---|---|---|---|
| Genotype and treatment | Neurons (*n*) | Mean ± SEM (pA) | *P* | Mean ± SEM (s) | *P* |
| mEPSC | | | | | |
| WT | 9 | 23.55 ± 0.99 | | 3.28 ± 0.65 | |
| WT+TTX | 10 | 37.66 ± 5.35 | < 0.01 | 1.52 ± 0.45 | < 0.05 |
| WT+CNQX/D-AP5 | 8 | 39.44 ± 4.76 | < 0.05 | 1.47 ± 0.32 | < 0.05 |
| WT+Bic | 11 | 19.82 ± 0.77 | < 0.05 | 2.27 ± 0.27 | > 0.05 |
| *Mecp2* KO | 14 | 34.26 ± 3.08 | < 0.01 | 1.79 ± 0.45 | < 0.05 |
| *Mecp2* KO+TTX | 10 | 35.41 ± 2.59 | > 0.05 | 0.72 ± 0.11 | < 0.05 |
| *Mecp2* KO+CNQX/D-AP5 | 10 | 36.00 ± 3.47 | > 0.05 | 1.52 ± 0.32 | > 0.05 |
| *Mecp2* KO+Bic | 11 | 34.88 ± 3.86 | > 0.05 | 1.34 ± 0.29 | > 0.05 |
| WT+EEA1 | 8 | 22.25 ± 0.30 | > 0.05 | 1.31 ± 0.20 | < 0.01 |
| *Mecp2* KO+EEA1 | 11 | 24.34 ± 0.91 | < 0.01 | 1.39 ± 0.37 | > 0.05 |
| *Mecp2* KO+EEA1+TTX | 13 | 22.07 ± 1.14 | > 0.05 | 1.30 ± 0.20 | >0.05 |
| *Mecp2* KO+EEA1+Bic | 10 | 19.21 ± 0.72 | < 0.01 | 1.63 ± 0.26 | > 0.05 |
| mIPSC | | | | | |
| WT | 15 | 36.40 ± 1.65 | | 1.16 ± 0.15 | |
| WT+TTX | 17 | 34.84 ± 1.92 | > 0.05 | 1.66 ± 0.32 | > 0.05 |
| WT+Bic | 19 | 42.36 ± 1.82 | > 0.05 | 1.03 ± 0.19 | > 0.05 |
| *Mecp2* KO | 13 | 36.32 ± 2.33 | > 0.05 | 1.19 ± 0.22 | > 0.05 |
| *Mecp2* KO+TTX | 12 | 36.48 ± 2.59 | > 0.05 | 1.43 ± 0.29 | > 0.05 |
| *Mecp2* KO+Bic | 13 | 38.54 ± 2.55 | > 0.05 | 2.18 ± 0.46 | > 0.05 |

**Table 2. Kinetics of mEPSCs**

| Genotype and treatment | Neurons (*n*) | Rise time (ms) | 10–90% rise time (ms) | Decay tau (ms) | Half-width (ms) | Charge transfer (pC) |
|---|---|---|---|---|---|---|
| WT | 9 | 2.19 ± 0.15 | 1.67 ± 0.14 | 4.67 ± 0.41 | 3.68 ± 0.37 | 106.01 ± 11.83 |
| WT+TTX | 10 | 2.05 ± 0.18 | 1.46 ± 0.20 | 4.64 ± 0.45 | 3.74 ± 0.35 | 150.93 ± 16.35* |
| WT+CNQX/D-AP5 | 8 | 2.27 ± 0.16 | 1.55 ± 0.18 | 5.33 ± 0.69 | 4.00 ± 0.44 | 169.64 ± 19.43* |
| WT+Bic | 11 | 2.19 ± 0.22 | 1.68 ± 0.19 | 4.59 ± 0.58 | 3.35 ± 0.41 | 89.38 ± 12.97 |
| *Mecp2* KO | 14 | 1.68 ± 0.19* | 1.13 ± 0.17* | 3.56 ± 0.46 | 2.93 ± 0.40 | 109.88 ± 19.51 |
| *Mecp2* KO+TTX | 10 | 1.60 ± 0.14 | 0.97 ± 0.12 | 3.54 ± 0.31 | 2.88 ± 0.19 | 110.19 ± 8.60 |
| *Mecp2* KO+CNQX/D-AP5 | 10 | 1.86 ± 0.14 | 1.16 ± 0.11 | 3.95 ± 0.33 | 3.14 ± 0.29 | 123.81 ± 13.35 |
| *Mecp2* KO+Bic | 11 | 1.97 ± 0.16 | 1.28 ± 0.16 | 4.54 ± 0.51 | 3.55 ± 0.39 | 130.43 ± 13.30 |
| WT+EEA1 | 8 | 1.88 ± 0.15 | 1.43 ± 0.15 | 4.12 ± 0.36 | 3.12 ± 0.28 | 82.21 ± 6.41 |
| *Mecp2* KO+EEA1 | 11 | 1.47 ± 0.09 | 1.04 ± 0.09 | 3.43 ± 0.22 | 2.53 ± 0.17 | 73.77 ± 6.35* |
| *Mecp2* KO+EEA1+TTX | 13 | 1.62 ± 0.08 | 1.17 ± 0.07 | 3.32 ± 0.11 | 2.41 ± 0.07 | 64.31 ± 1.98 |
| *Mecp2* KO+EEA1+Bic | 10 | 1.51 ± 0.08 | 1.09 ± 0.07 | 3.21 ± 0.12 | 2.21 ± 0.09 | 54.31 ± 2.80* |

*$P < 0.05$ compared to WT; neurons in TTX-, CNQX/D-AP5-, or Bic-treated cultures compared to their respective controls.

of the ionotropic glutamate receptor antagonists CNQX (10 $\mu$M) and D-AP5 (50 $\mu$M) ($n = 8$; mEPSC amplitude, $P < 0.05$; mEPSC frequency, $P < 0.05$; Table 1). In addition, chronic over-excitation by blockade of $GABA_A$R-mediated inhibition with bicuculline for 48 h significantly decreased mEPSC amplitude ($P < 0.05$). None of these chronic treatments altered mEPSC frequency and kinetics (Fig. 2 and Table 2; Ctl, $n = 9$; TTX, $n = 10$; bicuculline, $n = 11$; $P > 0.05$). On the other hand, mEPSC amplitude did not change in *Mecp2* KO neurons either after chronic silencing with TTX or CNQX/D-AP5, or after chronic blockade of $GABA_A$R-mediated inhibition with bicuculline (Fig. 2*A* and *B*; Ctl, $n = 14$; TTX, $n = 10$; CNQX/D-AP5, $n = 10$; bicuculline, $n = 11$; ANOVA, $P = 0.9685$). Intriguingly, *Mecp2* KO neurons did scale up mEPSC frequency after chronic inhibition of neuronal activity, but only when exposed to TTX (ANOVA, $P = 0.0462$; Dunnett's *post hoc* test, $P < 0.05$) and not CNQX/D-AP5 ($P > 0.05$; Table 1). The amplitude and the frequency of miniature inhibitory postsynaptic currents (mIPSCs) were not significantly different between *Mecp2* KO and WT neurons, and did not change after chronic silencing with TTX or over-excitation

with bicuculline (ANOVA WT amplitude, $P = 0.2776$; frequency, $P = 0.4026$; *Mecp2* KO amplitude, $P = 0.7796$; frequency, $P = 0.1212$; Table 1).

A key feature of HSP is that the amplitude distribution of mEPSCs is scaled by a multiplicative factor (Turrigiano *et al.* 1998; Soares *et al.* 2013). mEPSCs from neurons chronically silenced with TTX or disinhibited with bicuculline were rank-ordered by their amplitude and plotted against the rank-ordered mEPSC amplitudes from untreated control neurons (Fig. 3). The rank-order plots were fitted with straight lines to obtain the scaling factors in each genotype and homeostatic treatment. In WT neurons, mEPSCs scaled up by a factor of 1.58 after TTX silencing ($P < 0.0001$), whereas mEPSCs scaled down by a factor of 0.85 after bicuculline blockade of $GABA_AR$-mediated inhibition ($P < 0.0001$). On the other hand, mEPSC amplitudes showed a scaling factor of around 1 in *Mecp2* KO neurons after either TTX silencing or bicuculline blockade of $GABA_AR$-mediated inhibition, indicating a lack of homeostatic synaptic scaling. Consistent with higher synaptic GluA1 surface levels and larger mEPSCs, *Mecp2* KO neurons showed a scaling factor of 1.47 compared to WT neurons ($P < 0.0001$). These observations indicate that multiplicative homeostatic synaptic plasticity at excitatory synapses is impaired in *Mecp2* KO neurons.

The number of AMPAR channels and their mean conductance during quantal synaptic transmission were estimated by peak-scaled non-stationary noise analysis of mEPSCs (Soares *et al.* 2013) (Fig. 4*A* and *B*). This analysis indicates that larger mEPSC in *Mecp2* KO neurons reflect higher AMPAR channel conductance than in WT neurons (Fig. 4*D*; $P = 0.0046$). In WT neurons, chronic silencing with TTX significantly increased mean channel conductance (Fig. 4*D*; ANOVA, $P = 0.0199$; Dunnett's *post hoc* test, $P < 0.05$), without affecting channel number (Fig. 4*C*; ANOVA, $P = 0.0453$; Dunnett's *post hoc* test, $P > 0.05$). On the other hand, chronic over-excitation of WT neurons significantly decreased channel number (Fig. 4*C*; $P < 0.05$), without affecting channel conductance (Fig. 4*D*; $P > 0.05$). As observed with mEPSC amplitudes, neither chronic silencing with TTX (Fig. 4*D*; ANOVA, $P = 0.5487$) nor chronic over-excitation with bicuculline (Fig. 4*C*; ANOVA, $P = 0.5164$) affected channel conductance and channel number in *Mecp2* KO neurons.

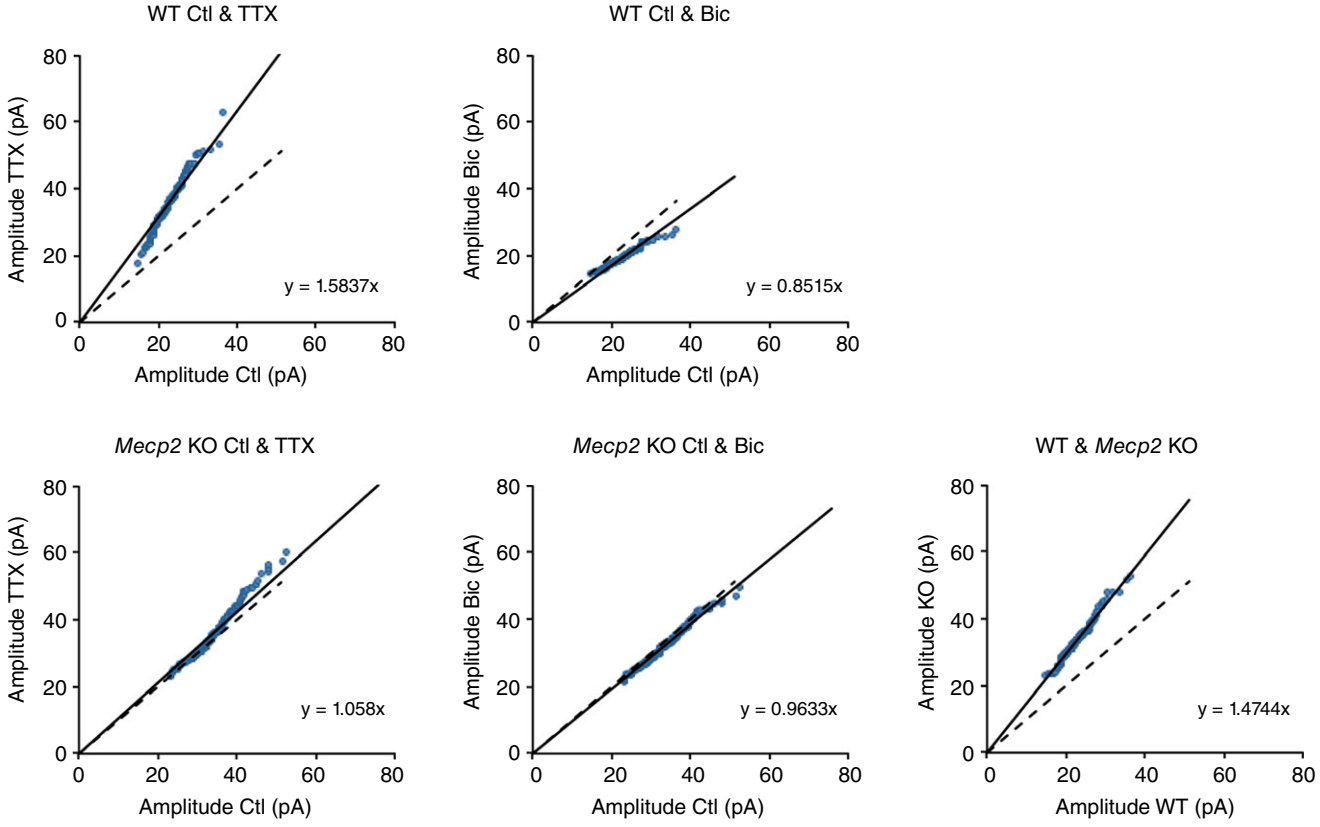


**Figure 3. *Mecp2* knockout neurons do not express homeostatic scaling of mEPSC amplitude**
Ranked-ordered mEPSC amplitudes from neurons in TTX- or bicuculline-treated cultures were plotted against rank-ordered mEPSC amplitudes from Ctl neurons. The multiplicative factor *y* was significantly larger than 1 in TTX-treated WT cultures, significantly smaller than 1 in bicuculline-treated WT cultures and not significantly different from 1 in *Mecp2* KO neurons. [Colour figure can be viewed at wileyonlinelibrary.com]

### Expression of EEA1 restores homeostatic synaptic plasticity in *Mecp2* KO neurons

Since surface levels of AMPARs at synapses depend on the relative rates of receptor exocytosis and endocytosis, the higher levels of GluA1 observed in *Mecp2* KO neurons could result from impaired AMPAR endocytosis. Interestingly, the gene encoding early endosome antigen 1 (EEA1), a protein that participates in AMPAR endocytosis, is down-regulated in hypothalamic samples from *Mecp2* KO mice (Chahrour *et al.* 2008). Consistently, the levels of EEA1 mRNA and protein were lower in the hippocampus, cortex, thalamus and brainstem of symptomatic *Mecp2* KO mice compared to age-matched WT controls (WT, $n = 5$, *Mecp2* KO, $n = 6$; Fig. 5).

Primary cultures of hippocampal neurons from neonatal *Mecp2* KO mice also have significantly lower levels of EEA1 mRNA and protein than WT neurons (WT, $n = 4$ cultures, *Mecp2* KO, $n = 4$; mRNA, $P = 0.0036$; protein, $P = 0.0130$; Fig. 6*A*). Transfection

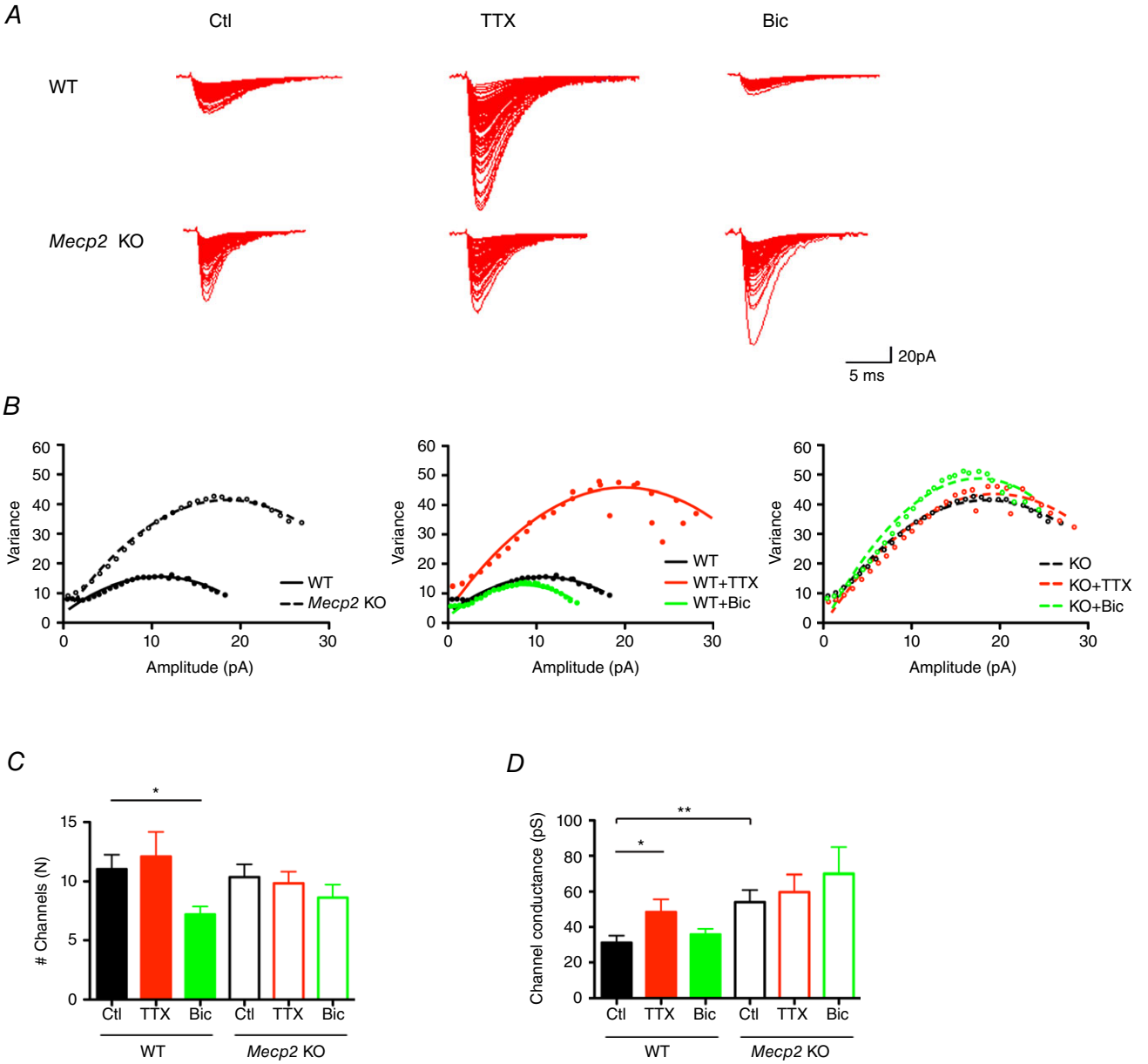


**Figure 4. Enhanced AMPAR channel conductance in *Mecp2* knockout neurons**
*A*, traces of mEPSC recordings from WT and *Mecp2* KO neurons in Ctl, TTX- or bicuculline-treated cultures (48 h). *B*, current–variance plots from peak-scaled non-stationary noise analysis of mEPSCs from WT and *Mecp2* KO neurons. *C*, number of channels open at the peak of cell-averaged mEPSCs from WT and *Mecp2* KO neurons. *D*, mean channel conductance for mEPSC recorded from WT and *Mecp2* KO neurons. $^*P < 0.05$; $^{**}P < 0.01$. [Colour figure can be viewed at wileyonlinelibrary.com]

of *Mecp2* KO neurons with a cDNA plasmid encoding EEA1 significantly increased its mRNA and protein levels, reaching those of WT neurons ($n = 3$ cultures; mRNA ANOVA, $P = 0.0042$; Tukey's *post hoc* test, $P < 0.01$; protein ANOVA, $P = 0.0097$; Tukey's *post hoc* test, $P < 0.05$; Fig. 6*A*). Increasing EEA1 levels in *Mecp2* KO neurons significantly reduced mEPSC amplitudes, which were comparable to WT levels ($n = 11$; ANOVA, $P = 0.0028$; Tukey's *post hoc* test, $P < 0.01$; Fig. 6*B* and *C*; Table 1); however, mEPSC frequency was not affected by EEA1 expression (ANOVA, $P = 0.0379$; Tukey's *post hoc* test, $P > 0.05$; Fig. 6*D*; Table 1). Furthermore, EEA1 expression in *Mecp2* KO neurons restored scaling down of mEPSC amplitude after chronic bicuculline blockade of $GABA_AR$-mediated inhibition ($n = 10$; ANOVA, $P = 0.0052$; Dunnett's *post hoc* test, $P < 0.01$; Fig. 6*B* and *E*; Table 1). Consistent with the recovery of only receptor endocytosis by EEA1 expression, scaling up mEPSC amplitudes in response to silencing with TTX was not recovered in EEA1-expressing *Mecp2* KO neurons(Fig. 6*B* and *E*; $n = 13$; $P > 0.05$; Table 1). Increasing EEA1 levels in WT KO neurons did not affect mEPSC amplitude ($n = 8$; $P = 0.1199$), but intriguingly increased mEPSC frequency ($n = 8$; $P = 0.0084$; Table 1). Taken altogether, these results indicate that EEA1-mediated endocytosis of GluA1 is impaired in *Mecp2* KO neurons, which results in larger mEPSCs that are unable to undergo activity-dependent homeostatic synaptic plasticity.

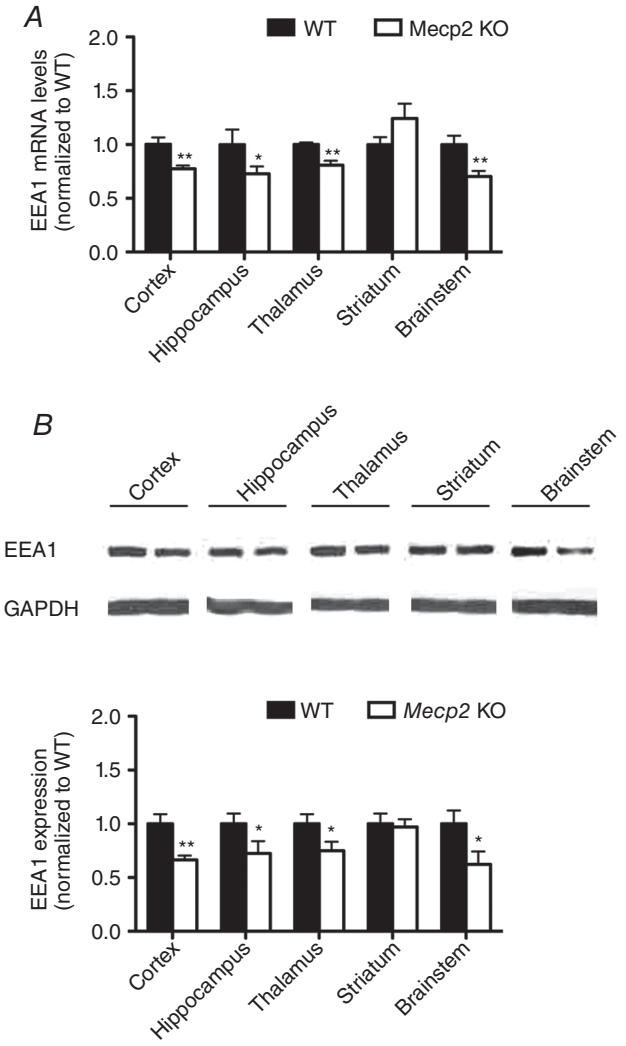


**Figure 5. EEA1 mRNA (*A*) and protein (*B*) levels in cortex, hippocampus, thalamus, striatum and brainstem from sympathetic *Mecp2* knockout mice and age-matched WT littermates**
All were normalized to that in WT mice. $^*P < 0.05$; $^{**}P < 0.01$.

## Discussion

Homeostatic synaptic scaling adjusts the strength of all synapses of a neuron up or down to stabilize neuronal circuits during positive feedback 'Hebbian' plasticity at specific synapses (Turrigiano *et al.* 1998; Turrigiano, 2008; Blackman *et al.* 2012; Qiu *et al.* 2012). The best understood mechanism for homeostatic synaptic scaling is the synaptic trafficking of AMPA-type glutamate receptors at excitatory synapses (Turrigiano *et al.* 1998; Turrigiano, 2008; Kim *et al.* 2012). Our results confirm that chronic silencing of hippocampal neurons with TTX increases both mEPSC amplitude and synaptic levels of GluA1, reflecting GluA1 insertion at synapses. In addition, chronic over-excitation by blockade of $GABA_AR$-mediated inhibition with bicuculline decreases both mEPSC amplitude and synaptic levels of GluA1. In addition to those postsynaptic changes, we observed homeostatic changes in the levels of the presynaptic protein VGLUT1 and in the frequency of mEPSCs, consistent with reports of homeostatic plasticity of presynaptic function (Murthy *et al.* 2001; Burrone *et al.* 2002; Thiagarajan *et al.* 2002; Erickson *et al.* 2006; Turrigiano, 2007). Reports of exclusive postsynaptic changes during homeostatic synaptic plasticity (Lissin *et al.* 1998; O'Brien *et al.* 1998; Turrigiano *et al.* 1998; Watt *et al.* 2000; Wierenga *et al.* 2005) may reflect differences in culture conditions or developmental stages (Wierenga *et al.* 2006), or the use of TTX or a cocktail of AMPA and NMDA receptor antagonists to silence neuronal activity (see below).

So far, the only studies of MeCP2's role in homeostatic synaptic plasticity are two reports that described the lack of synaptic scaling after shRNA-mediated knockdown of MeCP2 in cortical neurons: one study measured mEPSC and AMPAR levels after chronic bicuculline blockade of $GABA_AR$-mediated inhibition (Blackman *et al.* 2012; Qiu *et al.* 2012), and the other after chronic silencing with the AMPAR antagonist 6,7-dinitroquinoxaline-2,3-dione (DNQX; Blackman *et al.* 2012; Qiu *et al.* 2012). Here, we report that hippocampal neurons from *Mecp2* KO mice do

not express bidirectional homeostatic synaptic plasticity after either chronic silencing or chronic over-excitation. *Mecp2* KO neurons do not show the characteristic homeostatic scaling up of mEPSC amplitude and of synaptic levels of GluA1 after chronic silencing with TTX. Intriguingly, *Mecp2* KO neurons did show the characteristic scaling up of mEPSC frequency after chronic neuronal silencing, but only when exposed to TTX and not a combination of AMPA and NMDA receptor antagonists (CNQX/D-AP5). This apparent discrepancy is likely to reflect the different mechanisms by which TTX and CNQX/D-AP5 reduce neuronal activity: action potential-dependent presynaptic neurotransmitter release *vs.* postsynaptic glutamate receptor blockade, respectively. This difference

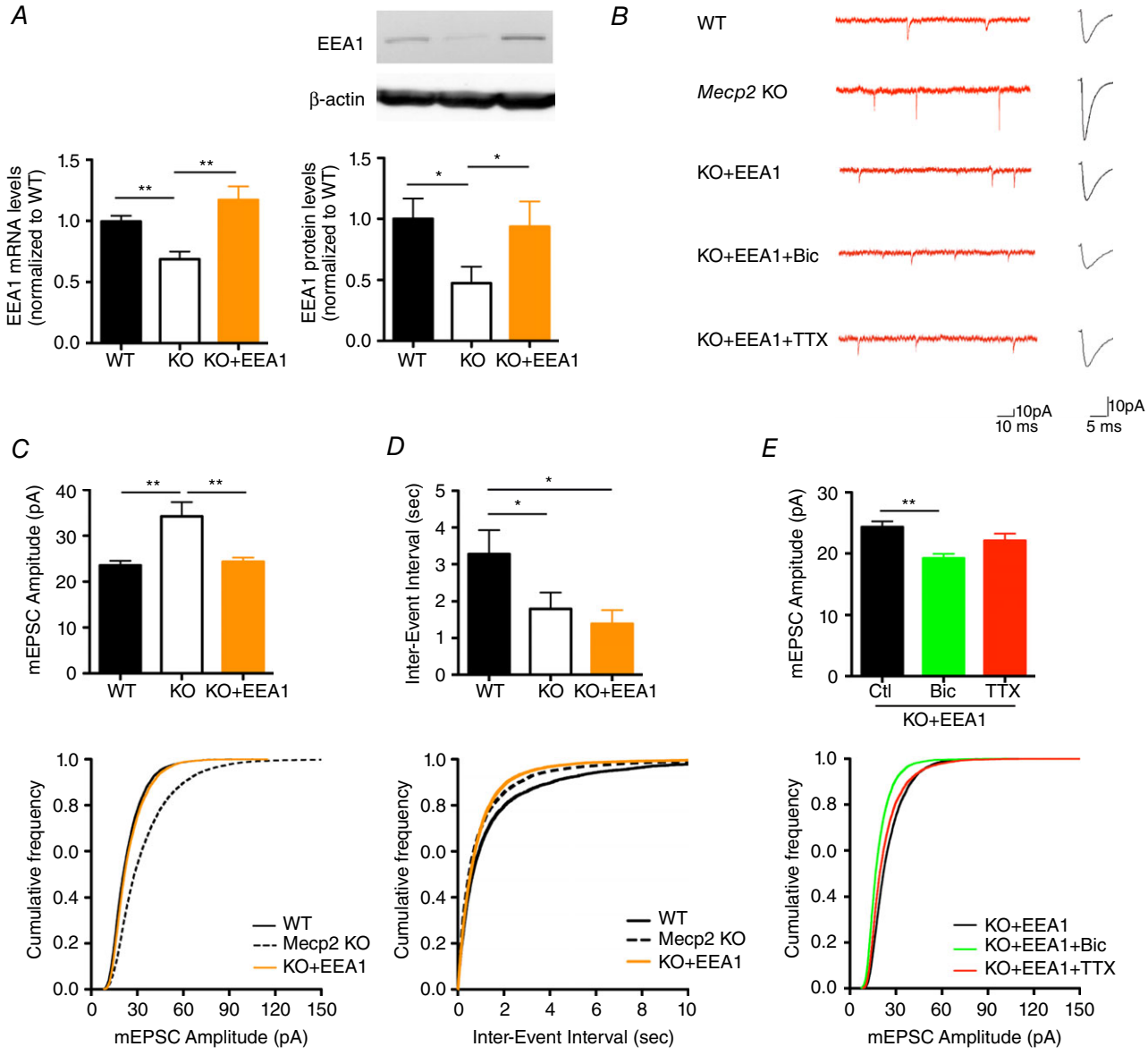


**Figure 6. EEA1 expression reduces mEPSC amplitude and restores their homeostatic scaling in *Mecp2* knockout neurons**
*A*, mRNA (left) and protein (right) levels of EEA1 in WT, *Mecp2* KO and *Mecp2* KO neurons after EEA1 expression. All were normalized to that in WT neurons. *B*, representative mEPSC recordings from WT, *Mecp2* KO and EEA1-expressing *Mecp2* KO neurons. *C*, average mEPSC amplitudes (for each cell) and cumulative probability distributions of mEPSC amplitudes from WT, *Mecp2* KO and EEA1-expressing *Mecp2* KO neurons. *D*, average mEPSC inter-event intervals (for each cell) and cumulative probability distributions of mEPSC inter-event intervals from WT, *Mecp2* KO and EEA1-expressing *Mecp2* KO neurons. *E*, average mEPSC amplitudes (for each cell) and cumulative probability distributions of mEPSC amplitudes from EEA1-expressing *Mecp2* KO neurons in Ctl, bicuculline-, or TTX-treated cultures. $^{*}P < 0.05$; $^{**}P < 0.01$. [Colour figure can be viewed at wileyonlinelibrary.com]

is critical because spontaneous TTX-insensitive miniature excitatory postsynaptic potentials (mEPSPs) transiently depolarize dendritic spines and dendrites during the 48 h TTX treatment period, while they are completely blocked by CNQX/D-AP5. Further studies are needed to define the role of spontaneous mEPSPs in homeostatic scaling of presynaptic function, and whether the cellular and molecular mechanisms at play are affected by *Mecp2* deletion.

The deficit in homeostatic synaptic plasticity is bidirectional because *Mecp2* KO neurons also fail to scale down mEPSC amplitude and synaptic levels of GluA1 after chronic over-excitation by bicuculline blockade of $GABA_AR$-mediated inhibition. Such disruption of homeostatic synaptic plasticity may lead to pathological increases in neuronal and network excitability, resulting in cognitive and neurological deficits in Rett individuals. Indeed, synapses of *Mecp2* KO neurons have significantly higher levels of surface GluA1 and presynaptic VGLUT1 than WT neurons. Consistently, mEPSCs are larger, more frequent and with higher channel conductance in *Mecp2* KO neurons, suggesting stronger synaptic strength, as observed in hippocampal slices from symptomatic mice (Li *et al.* 2016).

Changes in mEPSC amplitude are generally interpreted as changes in either receptor channel number or conductance (Turrigiano & Nelson, 2004). Our non-stationary noise analysis of AMPAR-mediated mEPSCs (Soares *et al.* 2013) indicates that chronic silencing enhanced receptor channel conductance without changing receptor channel number, while chronic over-excitation decreased receptpr channel number without affecting receptor channel conductance. It is unclear why TTX and bicuculline modified mEPSC amplitude by different mechanisms, but it has been reported that the signalling pathways involved in scaling up are not involved in scaling down (Turrigiano, 2008). The result of higher synaptic GluA1 levels after chronic silencing seems at odds with the lack of changes in receptor channel number. However, the homeostatic increase in AMPAR channel conductance results from an increase in the number of higher conductance GluA2-lacking AMPARs (Soares *et al.* 2013). Therefore, chronic silencing triggers a change in subunit composition of AMPARs favouring GluA1-only complexes, without changing the total number of receptor channels at the postsynaptic density.

A number of signalling pathways may be involved in the consequences of *Mecp2* deletion for homeostatic synaptic plasticity: brain-derived neurotrophic factor (BDNF), tumour necrosis factor $\alpha$ (TNF-$\alpha$) and Arc are all regulated by MeCP2 and have been proposed to participate in homeostatic scaling up after chronic silencing (Rutherford *et al.* 1998; Chen *et al.* 2003; Martinowich *et al.* 2003; Shepherd *et al.* 2006; Stellwagen & Malenka, 2006; Turrigiano, 2008; Su *et al.* 2012; O'Driscoll *et al.* 2015). On the other hand, activity-dependent phosphorylation of MeCP2 modulates synaptic strength and plasticity.

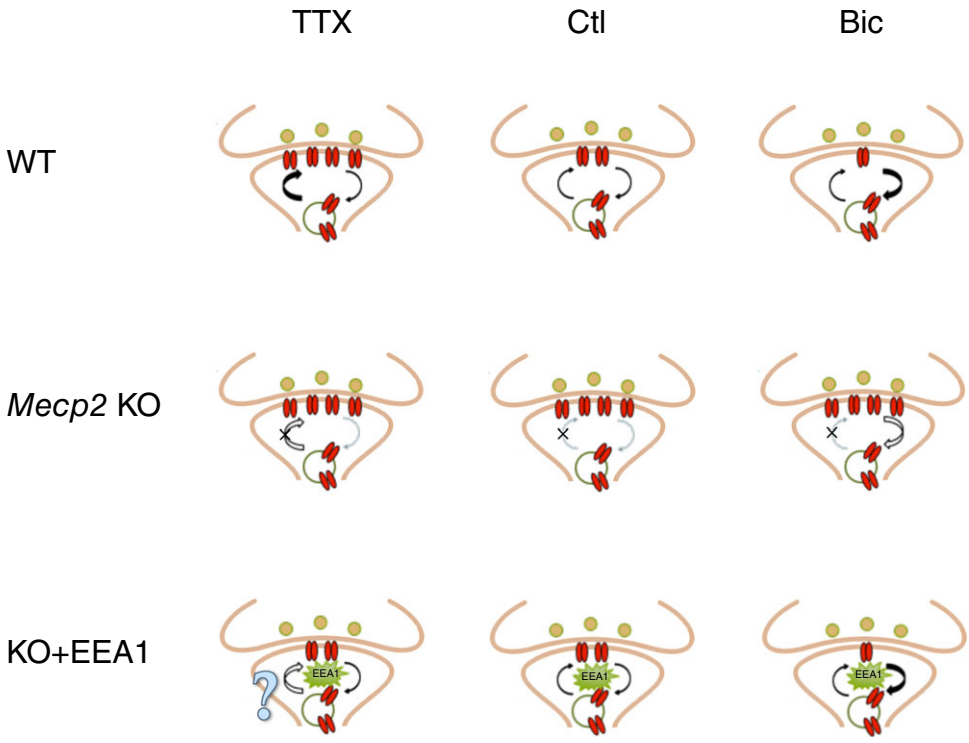


**Figure 7. Activity-dependent homeostatic regulation of AMPAR synaptic localization in wild-type and *Mecp2* knockout neurons**
[Colour figure can be viewed at wileyonlinelibrary.com]

Phosphorylation at S421 of MeCP2 is required for homeostatic scaling down after over-excitation with bicuculline (Zhong *et al.* 2012). MeCP2 may also participate in homeostatic synaptic scaling through activity-dependent gene transcription, since both scaling up and down require gene transcription (Ibata *et al.* 2008; Blackman *et al.* 2012).

The endosomal protein EEA1 is a critical factor controlling vesicle fusion during endocytosis via interacting with Rab5, *N*-ethylmaleimide-sensitive factor (NSF) and syntaxin13, and it is involved in AMPAR internalization (Mills *et al.* 1998; Simonsen *et al.* 1998; McBride *et al.* 1999; Lawe *et al.* 2002; Selak *et al.* 2006). An unbiased microarray study of hypothalamic samples found that EEA1 levels are lower in *Mecp2* KO mice (Chahrour *et al.* 2008). We found that the levels of EEA1 mRNA and protein are lower in several brain regions of *Mecp2* KO mice, suggesting impaired AMPAR endocytosis. Consistently, expression of EEA1 in *Mecp2* KO neurons reduced mEPSC amplitudes to wild-type levels, and restored homeostatic synaptic plasticity. These results are the first evidence that experimental manipulations of proteins involved in the activity-dependent trafficking of synaptic AMPA receptors restore synaptic function in Rett syndrome neurons, providing potentially novel targets of intervention for improving hippocampal function in RTT individuals.

Based on all these data, we proposed a working model (Fig. 7). In WT neurons under basal condition, insertion and endocytosis of AMPARs are balanced to maintain a stable level of receptors in the postsynaptic density. Chronic silencing leads to higher levels of AMPARs in the postsynaptic density by enhanced receptor insertion. Conversely, over-excitation increases receptor endocytosis, thus reducing surface levels of AMPARs. In *Mecp2* KO neurons, AMPARs reached a maximum level that cannot be further scaled up by chronic silencing. On the other hand, lower expression of endocytosis proteins such as EEA1 prevents scaling down in response to over-excitation. By expressing EEA1 in *Mecp2* KO neurons, AMPAR levels recovered back to wild-type levels, thus restoring scaling down in response to over-excitation by allowing AMPAR endocytosis. Further studies are required to identify the protein(s) involved in activity-dependent AMPAR insertion during homeostatic scaling up in response to chronic silencing.

In conclusion, our findings demonstrate that homeostatic synaptic plasticity at excitatory synapses is impaired in *Mecp2* KO neurons. In addition, EEA1 expression can restore homeostatic synaptic plasticity by allowing AMPAR endocytosis at excitatory synapses in *Mecp2* KO neurons. Our characterization of the role of EEA1 during homeostatic synaptic plasticity in *Mecp2* KO neurons provides potentially novel targets of intervention for improving hippocampal function in RTT individuals.

## References


Amaral MD & Pozzo-Miller L (2007). TRPC3 channels are necessary for brain-derived neurotrophic factor to activate a nonselective cationic current and to induce dendritic spine formation. *J Neurosci* **27**, 5179–5189.

Amir RE, Van Den Veyver IB, Wan M, Tran CQ, Francke U & Zoghbi HY (1999). Rett syndrome is caused by mutations in X-linked *MECP2*, encoding methyl-CpG-binding protein 2. *Nat Genet* **23**, 185–188.

Baj G, Patrizio A, Montalbano A, Sciancalepore M & Tongiorgi E (2014). Developmental and maintenance defects in Rett syndrome neurons identified by a new mouse staging system in vitro. *Front Cell Neurosci* **8**, 18.

Blackman MP, Djukic B, Nelson SB & Turrigiano GG (2012). A critical and cell-autonomous role for MeCP2 in synaptic scaling up. *J Neurosci* **32**, 13529–13536.

Burrone J, O'byrne M & Murthy VN (2002). Multiple forms of synaptic plasticity triggered by selective suppression of activity in individual neurons. *Nature* **420**, 414–418.

Calfa G, Hablitz JJ & Pozzo-Miller L (2011*a*). Network hyperexcitability in hippocampal slices from *Mecp2* mutant mice revealed by voltage-sensitive dye imaging. *J Neurophysiol* **105**, 1768–1784.

Calfa G, Percy AK & Pozzo-Miller L (2011*b*). Experimental models of Rett syndrome based on Mecp2 dysfunction. *Exp Biol Med (Maywood)* **236**, 3–19.

Calfa GLW, Rutherford JM, Pozzo-Miller L (2015). Excitation/inhibition imbalance and impaired synaptic inhibition in hipocampus area CA3 of *Mecp2* knockout mice. *Hippocampus* **25**, 159–168.

Chahrour M, Jung SY, Shaw C, Zhou X, Wong ST, Qin J & Zoghbi HY (2008). MeCP2, a key contributor to neurological disease, activates and represses transcription. *Science* **320**, 1224–1229.

Chao HT, Zoghbi HY & Rosenmund C (2007). MeCP2 controls excitatory synaptic strength by regulating glutamatergic synapse number. *Neuron* **56**, 58–65.

Chen RZ, Akbarian S, Tudor M & Jaenisch R (2001). Deficiency of methyl-CpG binding protein-2 in CNS neurons results in a Rett-like phenotype in mice. *Nat Genet* **27**, 327–331.

Chen WG, Chang Q, Lin Y, Meissner A, West AE, Griffith EC, Jaenisch R & Greenberg ME (2003). Derepression of BDNF transcription involves calcium-dependent phosphorylation of MeCP2. *Science* **302**, 885–889.

Erickson JD, De Gois S, Varoqui H, Schafer MK & Weihe E (2006). Activity-dependent regulation of vesicular glutamate and GABA transporters: a means to scale quantal size. *Neurochem Int* **48**, 643–649.

Faul F, Erdfelder E, Lang A.-G, & Buchner A (2007). G*Power 3: A flexible statistical power analysis program for the social, behavioral, and biomedical sciences. *Behavior Research Methods* **39**, 175–191.

Ibata K, Sun Q & Turrigiano GG (2008). Rapid synaptic scaling induced by changes in postsynaptic firing. *Neuron* **57**, 819–826.

Kim J, Tsien RW & Alger BE (2012). An improved test for detecting multiplicative homeostatic synaptic scaling. *PLoS One* **7**, e37364.

Lawe DC, Chawla A, Merithew E, Dumas J, Carrington W, Fogarty K, Lifshitz L, Tuft R, Lambright D & Corvera S (2002). Sequential roles for phosphatidylinositol 3-phosphate and Rab5 in tethering and fusion of early endosomes via their interaction with EEA1. *J Biol Chem* **277**, 8611–8617.

Li W, Xu X & Pozzo-Miller L (2016). Excitatory synapses are stronger in the hippocampus of Rett syndrome mice due to altered synaptic trafficking of AMPA-type glutamate receptors. *Proc Natl Acad Sci USA* **113**, E1575–E1584.

Lissin DV, Gomperts SN, Carroll RC, Christine CW, Kalman D, Kitamura M, Hardy S, Nicoll RA, Malenka RC & Von Zastrow M (1998). Activity differentially regulates the surface expression of synaptic AMPA and NMDA glutamate receptors. *Proc Natl Acad Sci USA* **95**, 7097–7102.

Martinowich K, Hattori D, Wu H, Fouse S, He F, Hu Y, Fan G & Sun YE (2003). DNA methylation-related chromatin remodeling in activity-dependent BDNF gene regulation. *Science* **302**, 890–893.

McBride HM, Rybin V, Murphy C, Giner A, Teasdale R & Zerial M (1999). Oligomeric complexes link Rab5 effectors with NSF and drive membrane fusion via interactions between EEA1 and syntaxin 13. *Cell* **98**, 377–386.

McGraw CM, Samaco RC & Zoghbi HY (2011). Adult neural function requires MeCP2. *Science* **333**, 186.

Mills IG, Jones AT & Clague MJ (1998). Involvement of the endosomal autoantigen EEA1 in homotypic fusion of early endosomes. *Curr Biol* **8**, 881–884.

Murthy VN, Schikorski T, Stevens CF & Zhu Y (2001). Inactivity produces increases in neurotransmitter release and synapse size. *Neuron* **32**, 673–682.

Nan X, Campoy FJ & Bird A (1997). MeCP2 is a transcriptional repressor with abundant binding sites in genomic chromatin. *Cell* **88**, 471–481.

Neul JL & Zoghbi HY (2004). Rett syndrome: a prototypical neurodevelopmental disorder. *Neuroscientist* **10**, 118–128.

O'brien RJ, Kamboj S, Ehlers MD, Rosen KR, Fischbach GD & Huganir RL (1998). Activity-dependent modulation of synaptic AMPA receptor accumulation. *Neuron* **21**, 1067–1078.

O'driscoll CM, Lima MP, Kaufmann WE & Bressler JP (2015). Methyl CpG binding protein 2 deficiency enhances expression of inflammatory cytokines by sustaining NF-$\kappa$B signaling in myeloid derived cells. *J Neuroimmunol* **283**, 23–29.

Percy AK & Lane JB (2005). Rett syndrome: model of neurodevelopmental disorders. *J Child Neurol* **20**, 718–721.

Qiu Z, Sylwestrak EL, Lieberman DN, Zhang Y, Liu XY & Ghosh A (2012). The Rett syndrome protein MeCP2 regulates synaptic scaling. *J Neurosci* **32**, 989–994.

Rutherford LC, Nelson SB & Turrigiano GG (1998). BDNF has opposite effects on the quantal amplitude of pyramidal neuron and interneuron excitatory synapses. *Neuron* **21**, 521–530.

Selak S, Paternain AV, Fritzler MJ & Lerma J (2006). Human autoantibodies against early endosome antigen-1 enhance excitatory synaptic transmission. *Neuroscience* **143**, 953–964.

Selak S, Woodman RC & Fritzler MJ (2000). Autoantibodies to early endosome antigen (EEA1) produce a staining pattern resembling cytoplasmic anti-neutrophil cytoplasmic antibodies (C-ANCA). *Clin Exp Immunol* **122**, 493–498.

Shepherd JD, Rumbaugh G, Wu J, Chowdhury S, Plath N, Kuhl D, Huganir RL & Worley PF (2006). Arc/Arg3.1 mediates homeostatic synaptic scaling of AMPA receptors. *Neuron* **52**, 475–484.

Simonsen A, Lippe R, Christoforidis S, Gaullier JM, Brech A, Callaghan J, Toh BH, Murphy C, Zerial M & Stenmark H (1998). EEA1 links PI(3)K function to Rab5 regulation of endosome fusion. *Nature* **394**, 494–498.

Soares C, Lee KF, Nassrallah W & Beique JC (2013). Differential subcellular targeting of glutamate receptor subtypes during homeostatic synaptic plasticity. *J Neurosci* **33**, 13547–13559.

Stellwagen D & Malenka RC (2006). Synaptic scaling mediated by glial TNF-$\alpha$. *Nature* **440**, 1054–1059.

Su D, Cha YM & West AE (2012). Mutation of MeCP2 alters transcriptional regulation of select immediate-early genes. *Epigenetics* **7**, 146–154.

Thiagarajan TC, Piedras-Renteria ES & Tsien RW (2002). $\alpha$- and $\beta$CaMKII: Inverse regulation by neuronal activity and opposing effects on synaptic strength. *Neuron* **36**, 1103–1114.

Turrigiano G (2007). Homeostatic signaling: the positive side of negative feedback. *Curr Opin Neurobiol* **17**, 318–324.

Turrigiano GG (2008). The self-tuning neuron: synaptic scaling of excitatory synapses. *Cell* **135**, 422–435.

Turrigiano GG, Leslie KR, Desai NS, Rutherford LC & Nelson SB (1998). Activity-dependent scaling of quantal amplitude in neocortical neurons. *Nature* **391**, 892–896.

Turrigiano GG & Nelson SB (2004). Homeostatic plasticity in the developing nervous system. *Nat Rev Neurosci* **5**, 97–107.

Wang G, Gilbert J & Man HY (2012). AMPA receptor trafficking in homeostatic synaptic plasticity: functional molecules and signaling cascades. *Neural Plast* **2012**, 825364.

Watt AJ, Van Rossum MC, Macleod KM, Nelson SB & Turrigiano GG (2000). Activity coregulates quantal AMPA and NMDA currents at neocortical synapses. *Neuron* **26**, 659–670.

Wierenga CJ, Ibata K & Turrigiano GG (2005). Postsynaptic expression of homeostatic plasticity at neocortical synapses. *J Neurosci* **25**, 2895–2905.

Wierenga CJ, Walsh MF & Turrigiano GG (2006). Temporal regulation of the expression locus of homeostatic plasticity. *J Neurophysiol* **96**, 2127–2133.

Zhong X, Li H & Chang Q (2012). MeCP2 phosphorylation is required for modulating synaptic scaling through mGluR5. *J Neurosci* **32**, 12841–12847.

## Additional information

### Competing interests

The authors do not have competing financial interests

### Author contributions

Both authors designed the experiments, analysed the data and wrote the manuscript. Both authors have approved the final version of the manuscript and agree to be accountable for all

aspects of the work. All persons designated as authors qualify for authorship, and all those who qualify for authorship are listed.

## Funding

This work was supported by Postdoctoral Fellowship IRSF-3177 (to X.X.) and NIH grants NS-065027 (to L.P.-M.).

## Acknowledgements

We thank Dr Wei Li for comments on the manuscript. We are indebted to Ms Lili Mao for mouse colony management and neuronal cultures, and Dr Takafumi Inoue (Waseda University, Tokyo) for data acquisition and analysis software.